

See discussions, stats, and author profiles for this publication at: <https://www.researchgate.net/publication/341936973>

# Automated MRI-Based Deep Learning Model for Detection of Alzheimer's Disease Process

Article in *International Journal of Neural Systems* · June 2020

DOI: 10.1142/S012906572050032X

CITATION

1

READS

124

11 authors, including:



**Nicholas Van Halm-Lutterodt**  
Capital Medical University

27 PUBLICATIONS 154 CITATIONS

[SEE PROFILE](#)



**Mohamed Mesregah**  
Keck School of Medicine USC

18 PUBLICATIONS 19 CITATIONS

[SEE PROFILE](#)



**Haibin Li**  
Capital Medical University

43 PUBLICATIONS 129 CITATIONS

[SEE PROFILE](#)



**Feng Zhang**  
Capital Medical University

19 PUBLICATIONS 116 CITATIONS

[SEE PROFILE](#)

Some of the authors of this publication are also working on these related projects:



Pathogenesis of Familial Cerebral Cavemous Malformation [View project](#)



my papers [View project](#)

## Automated MRI-Based Deep Learning Model for Detection of Alzheimer's Disease Process\*

Wei Feng

*Department of Epidemiology and Health Statistics, School of Public Health  
Capital Medical University, You'anmenwai, Xitoutiao No.10, Beijing, P. R. China  
Beijing Municipal Key Laboratory of Clinical Epidemiology  
Capital Medical University, Beijing, P. R. China  
sharkip@foxmail.com*

Nicholas Van Halm-Lutterodt

*Department of Neurosurgery, Beijing Tiantan Hospital  
Capital Medical University, Beijing, P. R. China  
Department of Orthopaedics and Neurosurgery  
Keck Medical Center of USC, Los Angeles, CA, USA*

Hao Tang

*School of Computer Science and Technology  
University of the Chinese Academy of Sciences, Beijing, P. R. China*

Andrew Mecum

*Department of Psychology, Emory University, Atlanta, GA, USA*

Mohamed Kamal Mesregah

*Department of Orthopaedics and Neurosurgery  
Keck Medical Center of USC, Los Angeles, CA, USA*

Yuan Ma, Haibin Li, Feng Zhang and Zhiyuan Wu

*Department of Epidemiology and Health Statistics, School of Public Health  
Capital Medical University, You'anmenwai, Xitoutiao No.10, Beijing, P. R. China  
Beijing Municipal Key Laboratory of Clinical Epidemiology  
Capital Medical University, Beijing, P. R. China*

Erlin Yao

*School of Computer Science and Technology  
University of the Chinese Academy of Sciences, Beijing, P. R. China*

Xiuhua Guo<sup>†</sup>

*Department of Epidemiology and Health Statistics, School of Public Health  
Capital Medical University, You'anmenwai, Xitoutiao No.10, Beijing, P. R. China  
Beijing Municipal Key Laboratory of Clinical Epidemiology  
Capital Medical University, Beijing, P. R. China  
statguo@ccmu.edu.cn*

---

<sup>†</sup>Corresponding author.

\*Data used in the preparation of this article were obtained from the Alzheimers disease neuroimaging initiative (ADNI) database (<http://adni.loni.usc.edu>). As such, the investigators within the ADNI contributed to the design and implementation of ADNI and/or provided data but did not participate in analysis or writing of this report. A complete listing of ADNI investigators can be found at [http://adni.loni.usc.edu/wp-content/uploads/how\\_to\\_apply/ADNI\\_Acknowledgement\\_List.pdf](http://adni.loni.usc.edu/wp-content/uploads/how_to_apply/ADNI_Acknowledgement_List.pdf).

Accepted 19 March 2020  
 Published Online 27 May 2020

In the context of neuro-pathological disorders, neuroimaging has been widely accepted as a clinical tool for diagnosing patients with Alzheimer's disease (AD) and mild cognitive impairment (MCI). The advanced deep learning method, a novel brain imaging technique, was applied in this study to evaluate its contribution to improving the diagnostic accuracy of AD. Three-dimensional convolutional neural networks (3D-CNNs) were applied with magnetic resonance imaging (MRI) to execute binary and ternary disease classification models. The dataset from the Alzheimer's disease neuroimaging initiative (ADNI) was used to compare the deep learning performances across 3D-CNN, 3D-CNN-support vector machine (SVM) and two-dimensional (2D)-CNN models. The outcomes of accuracy with ternary classification for 2D-CNN, 3D-CNN and 3D-CNN-SVM were  $82.57 \pm 7.35\%$ ,  $89.76 \pm 8.67\%$  and  $95.74 \pm 2.31\%$  respectively. The 3D-CNN-SVM yielded a ternary classification accuracy of 93.71%, 96.82% and 96.73% for NC, MCI and AD diagnoses, respectively. Furthermore, 3D-CNN-SVM showed the best performance for binary classification. Our study indicated that 'NC versus MCI' showed accuracy, sensitivity and specificity of 98.90%, 98.90% and 98.80%; 'NC versus AD' showed accuracy, sensitivity and specificity of 99.10%, 99.80% and 98.40%; and 'MCI versus AD' showed accuracy, sensitivity and specificity of 89.40%, 86.70% and 84.00%, respectively. This study clearly demonstrates that 3D-CNN-SVM yields better performance with MRI compared to currently utilized deep learning methods. In addition, 3D-CNN-SVM proved to be efficient without having to manually perform any prior feature extraction and is totally independent of the variability of imaging protocols and scanners. This suggests that it can potentially be exploited by untrained operators and extended to virtual patient imaging data. Furthermore, owing to the safety, noninvasiveness and nonirradiative properties of the MRI modality, 3D-CNN-SMV may serve as an effective screening option for AD in the general population. This study holds value in distinguishing AD and MCI subjects from normal controls and to improve value-based care of patients in clinical practice.

*Keywords:* Deep learning; convolution neural networks; three-dimensional magnetic resonance imaging; support vector machine; Alzheimer's disease; mild cognitive impairment.

## 1. Introduction

Alzheimer's disease (AD) reportedly accounts for nearly 60–70% of all cases of dementia<sup>1</sup> It currently remains a progressive neurodegenerative phenotype, affecting approximately 46.8 million people worldwide.<sup>2</sup> Affected persons critically demonstrate significant decline in cognitive function, greatly affecting their quality of life and overall health.<sup>3,4</sup> Unlike other neurological diseases, coping with AD has also demonstrated to be associated with a substantial burden of cost in Asia,<sup>5</sup> North America,<sup>6</sup> and even worldwide.<sup>7</sup> It has also been reported that by the year 2030, the worldwide estimated total cost of living with dementia will reach approximately 2.0 trillion USD.<sup>7</sup> Therefore, the focus of developing early interventional strategies to help prevent, diagnose, halt the progression and/or alleviate associated symptoms of dementia has become pertinent facets in both basic and clinical science research platforms.

One of the promising stages of the disease is 'mild cognitive impairment' (MCI), which is particularly recognized as a preclinical stage of AD that may serve as a target niche for early interventional strategies by potentially reverting, halting, or slowing down the accelerated progression of the disease.<sup>8</sup> Research studies are indicating that an approximation of 8–15% of MCI patients advance into AD stage annually,<sup>9</sup> while about 1–2% of individuals who were previously considered as healthy, acquired AD within the same given time-frame,<sup>10</sup> making early diagnosis an essential contributor of quality outcomes. Interestingly, evidence from the current literature shows that based on follow-up durations, the estimated incidences of reverting from the MCI stage to a normal state reportedly ranged from 4 to 15% in clinic-based studies and from 29 to 55% in population-based studies, respectively,<sup>11</sup> which further ascertains

that MCI a plausible interventional window stage to revert or halt the pathological progression of the disease process.

Neuro-imaging technology is an essential interventional strategy and diagnostic tool for the evaluation of neurological diseases.<sup>12,13</sup> As the brain remains a soft tissue organ, MRI proves to be the gold-standard neuro-imaging modality to evaluate its anatomic structural-to-functional alterations from the pathophysiological perspective.<sup>14–16</sup> In recent years, MRI has been the primary modality for AD diagnosis,<sup>2</sup> and MCI detection<sup>17,18</sup> due to its peculiar properties.<sup>19</sup> In the context of clinical screening of AD, the traditional MRI mode for the diagnostic classification of the disease has demonstrated relatively satisfactory outcomes for readily distinguishing between AD and normal controls, but MRI remains partially insensitive a technique for distinguishing between normal controls and MCI subjects.<sup>20</sup> Furthermore, as MRI features of MCI and AD subjects appear to be very similar, traditional imaging classifiers cannot effectively distinguish between the two stages of the disease, particularly in older age groups.<sup>21</sup> Therefore, this current study intended to evaluate the utility of artificial intelligence (AI)-based classification algorithms to address this limiting facet associated with the pathological distinction of the different stages involved in the disease process.

Machine learning and multivariate pattern analysis serve as powerful conventional tools for building image-based predictive models in computer-aided diagnostics.<sup>22</sup> Amongst patients with AD, the use of machine learning for individual-based diagnostic classification and clinical-score prediction has proven superior to traditional radiologic evaluation.<sup>3,23</sup> However, the image-related features required for machine learning cannot be extracted independently from the source by the machine itself, consequently requiring manual extraction by well-trained technicians, which clearly stands as a current limitation that consequently impacts efficiency outcomes in the screening of AD and MCI subjects.<sup>24</sup> This observed limitation prompts for a more efficient method that warrants early evaluation, detection and diagnoses of the pathologically staged spectra of AD.

Interestingly, deep learning methodology appears to be an advancement in the technology of computer-aided diagnostics. It mainly differs from machine

learning due to its requirement of little to no image pre-processing and can automatically integrate optimal representations of data from raw images without having to require any prior manual feature selection. The results of which are more objective, consistent and less bias-prone.<sup>25–27</sup> Convolutional neural network (CNN) is known as a sub-type of supervised deep learning method that has been recognized with great success in various medical fields, such as imaging and speech recognition, as well as natural language processing.<sup>28,29</sup> More importantly, CNN has proven to be the most effective algorithm for imaging-related AD diagnosis.<sup>30</sup> Most researchers have utilized CNN for binary classification based on two-dimensional (2D)-MRI for the diagnosis of AD,<sup>31</sup> but there are currently no established studies for the multi-classification of AD based on three-dimensional (3D)-CNN and solely MRI images.<sup>32</sup> Some researchers, nonetheless, did incorporate 3D-CNN-based MRI and positron emission tomography (PET) scans to diagnose AD regardless of the possible harm of irradiation exposure.<sup>33</sup> It is clear that the use of PET scans poses health risks, especially in vulnerably aged populations, and may not be suitable for screening AD in such populations.

Based on previous research, we found that support vector machine (SVM) is considered as the better classifier to the Softmax.<sup>34</sup> In this current study, our goal was to establish a classification model utilizing 3D-CNN with the aid of SVM and solely MRI samples, which shows direct automated extraction of features based on available imaging data.

## 2. Material and Methods

### 2.1. Database

All cases included in this study were collected at baseline from the Alzheimer’s disease neuroimaging initiative (ADNI) database with tests results and imaging outcomes comprising at least two years of follow-up. Complete patient information including demographic information, level of disease status, ancillary tests and other associated factors were summarized. In this study, a subset of 469 subjects having a total of 3127 MRI samples that contained structural 3T T1-weighted images and their respective anatomical segmentations from the ADNI dataset were used. 3T T1-weighted MRI samples were collected using 3D MPRAGE sequences, and

the diagnosis of each image sample was from a professional radiologist, as described in the ADNI acquisition protocol.<sup>35</sup> We randomly assigned the samples according to the proportion of 85% in the training group and 15% in the validation group and ensured that the proportion of patients in the two groups was similar. So, a total number of 398 subjects (NC = 135, MCI = 133, AD = 130) with 2544 image samples were distributed in the training group while a total number of 71 subjects (NC = 24, MCI = 24, AD = 23) with 469 image samples were designated as the validation group.

The research study proposed statistical method to compare basic information, recognition tests, serum and cerebrospinal fluid (CSF)  $A\beta$ , p-Tau and Tau protein levels in three groups (AD, MCI and NC). The differences between three groups for quantitative data were tested with analysis of variance (ANOVA), pairwise comparison test adopted LSD; for qualitative data were tested with the chi-square test ( $\alpha = 0.05$ ). Statistical analysis was performed using SPSS version 25.0 (IBM Corp., Armonk, NY). Statistical significance was set at  $P < 0.05$ .

## 2.2. Image pre-processing

The Think Server TS560 with Linux (Ubuntu 16.10) operating system was used for MRI pretreatment and CNN programs, including high-performance GPU NVIDIA Tesla P40, with 3840 CUDA cores and High-Frequency Intel Xeon E5-2650 V4 with 128 GB overall memory. All methods were implemented in Python version 2.7.12. The neural network is built by using the Keras library in deep learning based on TensorFlow. The analysts were blinded with the information of all subjects while performing the imaging data analysis.

To enhance standardization for MRI data, which needs a few steps to pre-process as follows; all MRI data were first spatially normalized by Statistical Parametric Mapping12 (SPM12)<sup>36</sup> to guarantee that each image voxel corresponded with the same anatomical position. Then, the skull and cervical parts in the imaging were stripped by using the Computational Anatomy Toolbox12 (CAT12),<sup>37</sup> an extended toolbox of SPM12. The voxel-based morphometric (VBM)<sup>38</sup> method was used by CAT12 to create a grey matter template. In addition, all MRI images were segmented to grey matter (GM), white

matter (WM) and CSF. The nonlinear affine transition was used to select and register GM images for the GM ICBM-152 standard template.

All 3D GMs were averaged and resized to  $96 \times 96 \times 96$  voxels with voxel-sizes of 1.5 mm (Sagittal)  $\times$  1.5 mm (Coronal)  $\times$  1.5 mm (axial) and concatenated into a stack. The Gaussian kernel was used to smoothen the stack, which approximately resulted in full width at half maximum (FWHM) of 7 mm. Considering the middle of the stack, 62 slices, contains thalamus, hippocampus and other important brain tissue about memory, our study used these ( $62 \times 96 \times 96$ ) to train the 3D-CNN. For 2D-CNN, only axial slices in the axial plane were used to train the parameters, which means that each subject provides 62 slices labeled for the same class regardless of spatial information.

## 2.3. Convolution neural networks

In this study, CNN, which is a kind of deep learning method, was used to extract the features from MRI imaging. CNN imitates the visual system of human beings to memorize and learn the edges and features of the graphics, so as to achieve the most effective recognition effect of such graphics.<sup>39</sup> Three special attributes of CNN are local connectivity, parameter sharing and invariant representation, which greatly reduce the computational complexity and thus simplify the network.

The main structures of CNN include a convolutional layer, pooling layer, fully connected layer and classifier. The convolutional layer was used to extract image features, which could generate the feature maps. The pooling layer was used to reduce the number of features from the convolutional layer. After the feature maps were optimally minimized, we reduced and transferred the feature maps into a column feature map, which in turn simplifies the parameter into an optimal number. Then, the classifiers were finally used for AD detection.

Based on the mathematical illustration in a previously reported study,<sup>40</sup> we based our current study on the differences between 2D and 3D CNNs. 2D and 3D CNNs use 2D and 3D convolutional kernels, respectively, to classify MRI scans based on slices (for 2D CNNs), or on volumetric patches (for 3D CNNs). In 2D CNNs, a full volume of MRI predictions is initially taken one-slice at a time while

the convolutional kernels achieve the necessary slice measurements of height and width to enable classification. Nevertheless, 2D-CNNs can only use single slices as inputs; they cannot supply context from connected slices. This implies that the predictions of MRI scans could be achieved by voxel information via connected slices.

3D CNNs resolve this problem by using 3D convolutional kernels to classify volumetric patches of scans. Leveraging inter-slice information can lead to improved performance, but this comes at an increased computational cost, since these CNNs utilize numerous parameters.

In 2D convolution, the activation value at spatial position  $(x, y)$  in the  $j$ th feature map of the  $i$ th layer, denoted as  $v_{i,j}^{x,y}$ , is generated using the following equation:

$$v_{i,j}^{x,y} = \phi \left( b_{i,j} + \sum_{\tau=1}^{d_{l-1}} \sum_{\rho=-\gamma}^{\gamma} \sum_{\sigma=-\delta}^{\delta} \omega_{i,j,\tau}^{\sigma,\rho} v_{i-1,\tau}^{x+\sigma,y+\rho} \right), \quad (1)$$

where  $\phi$  is the rectified linear unit (ReLU) activation function,  $b_{i,j}$  is the bias parameter for the  $j$ th feature map of the  $i$ th layer,  $d_{l-1}$  is the number of feature map in  $(l-1)$ th layer and the depth of kernel  $w_{i,j}$  for the  $j$ th feature map of the  $i$ th layer,  $2\gamma+1$  is the width of kernel,  $2\delta+1$  is the height of kernel and  $w_{i,j}$  is the value of weight parameter for the  $j$ th feature map of the  $i$ th layer.<sup>41</sup>

The 3D convolution is a process to form a cube by stacking multiple consecutive frames and then applying 3D convolution kernel in the cube. In 3D convolution, the activation value at spatial position  $(x, y, z)$

in the  $j$ th feature map of the  $i$ th layer, denoted as  $v_{i,j}^{x,y,z}$ , is generated as follows:

$$v_{i,j}^{x,y,z} = \phi b_{i,j} + \sum_{\tau=1}^{d_{l-1}} \sum_{\lambda=-\eta}^{\eta} \sum_{\tau=1}^{d_{l-1}} \sum_{\rho=-\gamma}^{\gamma} \sum_{\sigma=-\delta}^{\delta} \omega_{i,j,\tau}^{\sigma,\rho,\lambda} v_{i-1,\tau}^{x+\sigma,y+\rho,z+\lambda} \quad (2)$$

$2\eta+1$  is the depth of kernel along spectral dimension and other parameters are the same as in Eq. (1).<sup>42</sup> In brief, 3D CNN is an extension of 2D CNN. The 3D CNN uses the third dimension to store the temporal information from image sequences. Contrary to the 2D CNN, the 3D CNN retains a more computational complexity due to the additionally added level of dimension.

As shown in Figs. 1 and 2, processed MRI imaging of three planes was put in the first layer as the input layer in our experiment. And then,  $560 \ 3 \times 3 \times 3$  sized convolutional kernels were used to extract the features from the MRI imaging. The ReLU and batch normalization (BN) were put with the convolutional kernel to ensure more efficient gradient descent and simplified calculation process. Afterward, a  $560 \ 2 \times 2 \times 2$  sized max pooling, BN and ReLU were put in the pooling layer to reduce the parameters of feature maps. These steps were repeated four times to get streamlined feature maps. At the second pooling layer, we made the dropout function here decreases by half the number of neurons in CNN to simplify the architecture and to guarantee a higher computing speed. Then, the feature maps were compatibly created into fully connected layer by the ReLU and dropout function. At last, we used two classi-

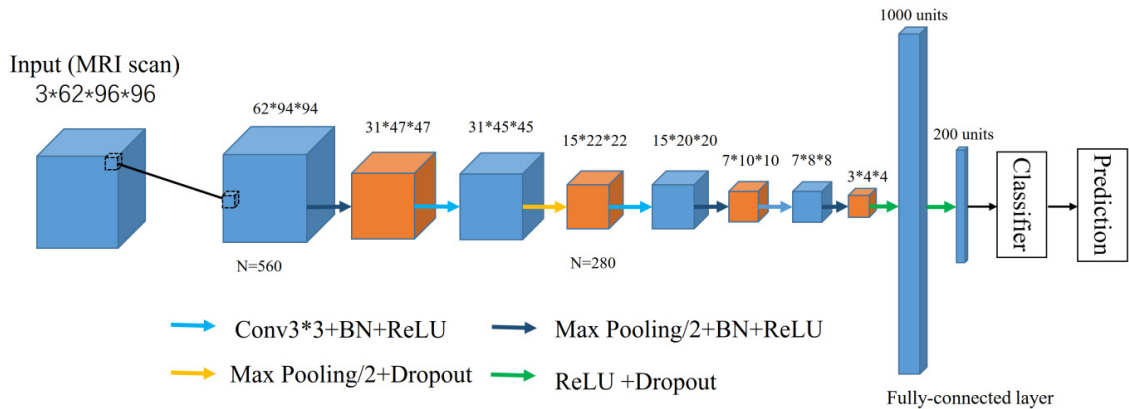


Fig. 1. The overall architecture for 3D-CNN adopted in this study.

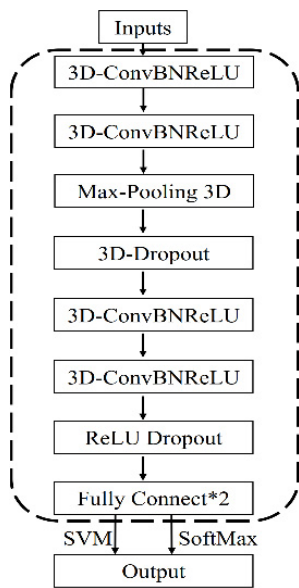


Fig. 2. The flowchart of the proposed for 3D-CNN adopted in this study.

Table 1. °The parameters are used in the 3D and 2D CNN.

Model	Function	Kernel size
3D-CNN	Convolutional kernels	$3 \times 3 \times 3$
3D-CNN	Max pooling	$2 \times 2 \times 2$
2D-CNN	Convolutional kernels	$3 \times 3$
2D-CNN	Max pooling	$2 \times 2$

fiers combined with 3D-CNN, one is Softmax and the other is SVM. However, SVM was considered as the better classifier to the Softmax from prior study.<sup>34</sup> The parameters used in the 3D and 2D CNN are shown in Table 1.

SVM is a widely applied supervised machine learning method aiming to solve binary classification problem. The mechanism of SVM is mapping nonlinear data into high dimensional space by kernel function and obtaining optimal classification plane for separating the individuals accurately. In this research, SVM used radial basis function (RBF) kernel (Gaussian kernel),  $C = 0.9$ . Standard 10-fold cross-validation was employed for training SVM with image features extracted by CNN to optimize the parameters (gamma and cost), which is not time-consuming and can obtain higher accuracy.<sup>43</sup> We used 3D-CNN to create binary (AD/NC, AD/MCI and MCI/NC) and ternary (AD, MCI and NC)

classifications. The 2D-CNN was also proposed to address the above questions for comparison with 3D-CNN. The CNN was trained by back-propagation (BP) algorithm with mini-batch gradient descent. The weights of the hidden layer and the output layer were randomly initialized.

## 2.4. Performance evaluation

The above three kinds of CNN models were trained for 50 epochs to ensure the best execution model and with the lowest value of objective function after training, and its performance was evaluated on the validation group. Specificity, sensitivity, accuracy and receiver operating characteristic curves (ROCs) and area under curves (AUCs) were used for presenting the differences between 2D-CNN and 3D-CNN-SVM and finding out which approach yielded the most efficient and reliable outcome. All accuracy, sensitivity and specificity results for binary classification were reported at the optimal operating point of the ROC.

## 3. Results

We found no significant differences in age and gender among the three groups, as shown in Table 2. Years of education, Minimum Mental State Examination (MMSE), Alzheimer’s Disease Assessment Scale-cognitive subscale (ADAS11) and ADAS13 were significantly different in the three groups, but not in NC and MCI. The concentration of Tau, p-Tau and  $A\beta$  is not only different in a three groups comparison but also in a pairwise comparison.

Results are shown in Table 3, expressing binary classification accuracy, sensitivity and specificity of AD. The performance of ternary classification’s accuracy for 2D-CNN, 3D-CNN and 3D-CNN-SVM was  $82.57 \pm 7.35\%$ ,  $89.76 \pm 8.67\%$  and  $95.74 \pm 2.31\%$ , respectively. The performance in ternary classification of 3D-CNN-SVM was significantly better than others ( $P < 0.05$ ). The 3D-CNN-SVM yielded the best performance relative to other methods for binary classification ( $P < 0.05$ ). Our study indicated that ‘NC versus MCI’ showed accuracy, sensitivity and specificity of 98.90%, 98.90% and 98.80%; ‘NC versus AD’ showed accuracy, sensitivity and specificity of 99.10%, 99.80% and 98.40%; and ‘MCI versus AD’ showed accuracy, sensitivity and specificity of 89.40%, 86.70%, and 84.00%, respectively;

Table 2. Basic information and cognitive indicators of the individuals in this study.

Index	NC ( $n = 159$ )	MCI ( $n = 157$ )	AD ( $n = 153$ )	$F/X^2$	$P$
Age	$75.16 \pm 4.12$	$74.81 \pm 8.15$	$74.17 \pm 8.21$	0.78	0.457
Number of male participants	65 (40.88)	106 (67.52)	53 (34.64)	10.41	0.600
Education	$16.21 \pm 2.15^a$	$15.51 \pm 3.40^c$	$14.31 \pm 3.15$	16.55	$< 0.001$
MMSE	$28.38 \pm 2.75^a$	$27.58 \pm 3.82^c$	$23.08 \pm 2.15$	141.13	$< 0.001$
ADAS11	$5.75 \pm 2.27^a$	$6.14 \pm 4.21^c$	$17.77 \pm 5.39$	420.53	$< 0.001$
ADAS13	$12.54 \pm 3.25^a$	$14.12 \pm 8.10^c$	$28.12 \pm 6.07$	278.11	$< 0.001$
Tau, pg/mL	$221.09 \pm 75.13^{ab}$	$293.09 \pm 116.63^c$	$355.49 \pm 112.72$	66.544	$< 0.001$
P-Tau, pg/mL	$20.37 \pm 7.59^{ab}$	$28.24 \pm 13.02^c$	$36.04 \pm 12.08$	77.29	$< 0.001$
$A\beta$ , pg/mL	$1056.52 \pm 407.33^{ab}$	$760.53 \pm 354.99^c$	$601.477 \pm 177.59$	76.79	$< 0.001$

Notes: Quantitative data were expressed as mean  $\pm$  standard deviation; qualitative data were expressed as number (percentage). MMSE: Mini-Mental State Examination; ADAS: Alzheimer’s Disease Assessment Scale-cognitive subscale; Tau: Tau protein in Cerebrospinal Fluid (CSF); P-Tau: Phosphorylated Tau protein in CSF;  $A\beta$ : Amyloid  $\beta$ -protein in CSF. Statistically positive significant results at the 5% level ( $P < 0.05$ ) are indicated in bold. <sup>a</sup>NC versus AD is statistically significant; <sup>b</sup>NC versus MCI is statistically significant; <sup>c</sup>MCI versus AD is statistically significant.

Table 3. The comparison for accuracy, sensitivity, and specificity of three kinds of binary classification for different CNN models.

Classification	Model	Accuracy(%)	Sensitivity(%)	Specificity(%)
AD versus NC	2D-CNN	$88.90 \pm 4.50$	$84.70 \pm 7.30$	$87.10 \pm 4.50$
	3D-CNN	$89.40 \pm 2.20$	$82.10 \pm 7.30$	$84.70 \pm 4.10$
	3D-CNN-SVM	<b><math>99.10 \pm 1.13</math></b>	<b><math>99.80 \pm 0.37</math></b>	<b><math>98.40 \pm 1.17</math></b>
AD versus MCI	2D-CNN	$65.20 \pm 3.40$	$62.40 \pm 3.50$	$67.90 \pm 9.10$
	3D-CNN	$86.50 \pm 2.70$	$74.00 \pm 4.20$	$78.90 \pm 9.10$
	3D-CNN-SVM	<b><math>89.40 \pm 6.90</math></b>	<b><math>86.70 \pm 9.10</math></b>	<b><math>84.00 \pm 4.80</math></b>
MCI versus NC	2D-CNN	$61.80 \pm 6.90$	$55.20 \pm 8.40$	$70.30 \pm 9.83$
	3D-CNN	$81.20 \pm 5.30$	$74.70 \pm 8.30$	$80.30 \pm 9.83$
	3D-CNN-SVM	<b><math>98.90 \pm 2.78</math></b>	<b><math>98.90 \pm 3.69</math></b>	<b><math>98.80 \pm 0.63</math></b>
Ternary Classification	2D-CNN	$82.57 \pm 7.35$	N/A	N/A
	3D-CNN	$89.76 \pm 8.67$	N/A	N/A
	3D-CNN-SVM	<b><math>92.11 \pm 2.31</math></b>	N/A	N/A

Notes: For each classification, the bolded outcomes represented robust significance of the SVM model compared to the outcomes of the other two models ( $P \leq 0.05$ ) N/A: Not applicable to Sensitivity and Specificity with respect to ternary classification.

however, the performance of the classification for AD and MCI was not effective. Softmax was used as a classifier in 2D-CNN with a very poor performance in all the binary and ternary classifications of AD.

AUC is shown in Fig. 3 and Table 4 of ROC. 3D-CNN-SVM had the highest AUC in the binary classification ( $P < 0.05$ ), AD versus MCI and MCI versus NC, making the AUC of binary classification 0.930 (0.875–0.985) and 0.998 (0.995–1.000), respectively.

Figure 4 illustrates the performance of multi-classification by 3D-CNN-SVM in the different development processes for AD, yielding 95.74% accuracy. The diagonal represents the number of correct predictions. The performance of ternary classification showed that the 3D-CNN-SVM acquired accuracy scores of 93.71%, 96.82% and 96.73% for NC, MCI and AD diagnoses, respectively. We found that the 3D-CNN-SVM was less effective in discriminating between NC and MCI.

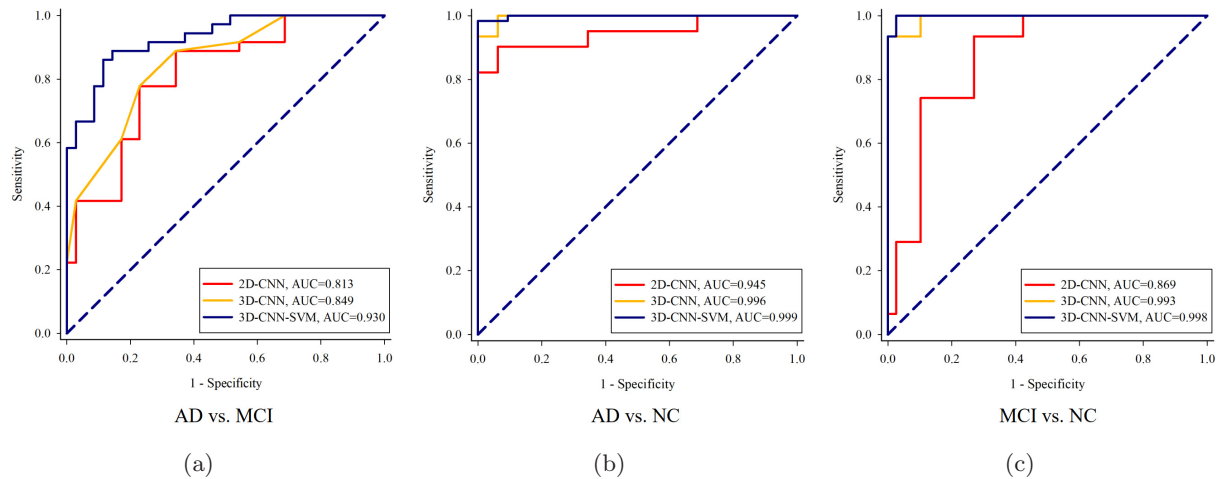


Fig. 3. Receiver Operating Characteristic Curve (ROC) for three different kinds of Deep Learning Model in AD Binary Classification.

Table 4. The comparison of AUC (95% CI) for binary classification in AD with different CNN models.

Classification	Model	AUC (95%CI)
AD versus NC	2D-CNN	0.945 (0.8874–1.000)
	3D-CNN	0.996 (0.988–1.000)
	3D-CNN-SVM	0.999 (0.995–1.000)
AD versus MCI	2D-CNN	0.813 (0.713–0.912)
	3D-CNN	0.849 (0.763–0.936)
	3D-CNN-SVM	<b>0.930 (0.875–0.985)</b>
MCI versus NC	2D-CNN	0.869 (0.788–0.949)
	3D-CNN	<b>0.993 (0.982–1.000)</b>
	3D-CNN-SVM	<b>0.998 (0.995–1.000)</b>

Note: For each classification, the bolded outcomes represent robust significance of specific models ( $P < 0.05$ ).

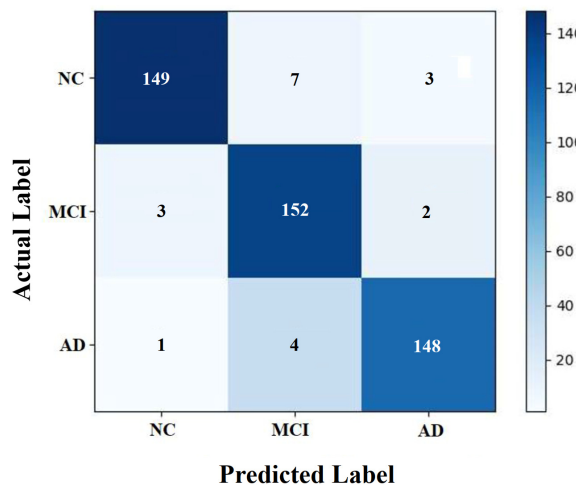


Fig. 4. Confusion Matrix for 3D-CNN-SVM Model in Ternary Classification's Performance.

Although the high performance of ternary classification was achieved by the new combination model (3D-CNN-SVM), overfitting may cause a reduction of performance when the model is used in other imaging databases. Figure 5 shows the accuracy of the training and validation group across the model utilizing structural MRI as inputs, which also achieved the highest classification accuracy. It can be found that the curves of the accuracy are almost the same in the training and validation group, illustrating comparable performance during both training and validation, therefore no significant overfitting.

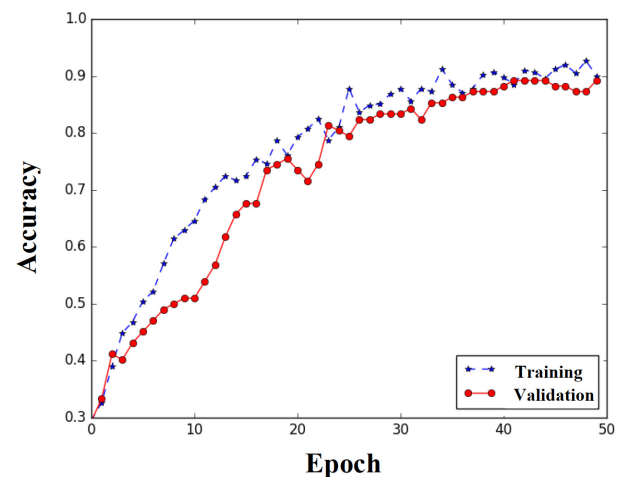


Fig. 5. The Iterative Graph of the Training and Validation Accuracy for Ternary Classification in 3D-CNN-SVM Model.

#### 4. Discussion

At present, morphological analyses of medical imaging scans are operated manually by skilled radiologists and imaging technicians, which can potentially result in reduced efficiency and inaccuracy, as well as overdependence on the analyst's skills.<sup>34</sup> Previous work indicates the potential clinical significance of CNN application in AD screening and detection.<sup>43,44</sup> However, brain MRI and ternary classification are yet to be considered in this area of work.<sup>45</sup> In the current study, we designed and trained a patterned classification system combining 3D-CNN and SVM for ternary classification. Our experimental outcome indicates that the performance of 3D-CNN is superior to 2D-CNN, whereas the expression with 3D-CNN-SVM yielded the best algorithm for binary and ternary classification of AD. More importantly, 3D-CNN-SVM performed appreciably well without any prior feature engineering and was completely independent of the variability of imaging protocols and scanner. This suggests that it could be utilized by untrained operators and potentially generate analyses of patient-imaging data with higher efficiency and greatly minimized technical errors.

Certain risk factors aside neuro-imaging have generally been implicated in the pathological role of AD such as patient's educational level,<sup>46</sup> age,<sup>47</sup> gender,<sup>48</sup> cognitive and mental status<sup>49</sup> as well as CSF total-tau (t-Tau), phosphorylated-tau (p-Tau) and amyloid-beta ( $A\beta$ ) proteins.<sup>50</sup> In this current study, we found that the analyses of the number of years of education, MMSE, ADAS11 and ADAS13 showed no differences across MCI and NC subjects, implying that the detection of MCI may be less sensitive with those clinical variables, probably due to the fine transitional line between normal control status and MCI stage. The concentrations of CSF t-Tau, p-Tau and  $A\beta$  are not only different across the three groups but also in pairwise comparison. There has been quite a number of reported evidence, where authors utilized CSF t-Tau, p-Tau and  $A\beta$  as important training data to increase the performance of their diagnostic models.<sup>51,52</sup> However, these diagnostic modalities may have downsides, due to their potentially harmful effects on health. A critical goal of computer-aided diagnosis in the field of neuro-imaging is to improve the approach to the diagnoses of neurological diseases by means of utilizing less invasive

means, and if possible, nonirradiating neuroimaging modality.<sup>53,54</sup> To effectively address this needed area of technology into clinical practicum, we needed to incorporate a method to clearly distinguish between AD, MCI and NC in an easier, safer and efficient way.

Since the invention of the MRI, its application has rapidly gained irreplaceable grounds as a gold-standard for soft tissue imaging.<sup>55</sup> This can be attributed to its pertaining properties of nonirradiation and noninvasiveness as well as weighted-signal intensities to tissue and fluid,<sup>56</sup> which warrant this imaging modality for the replicable screenings of neurological diseases. Based on these imaging properties, MRI scans were proposed in this study as the training data for CNN to classify MCI and AD subjects from NC subjects.

Automated classification with different image-extracting features is an important step in the analysis of structural to functional morphology in MRI technology. The traditional diagnosis of AD is usually based on manual extraction of texture features, which requires an impractical amount of time and human resource for image pre-processing.<sup>57</sup>

In special circumstances, some pathological atrophic changes that occur in certain cerebral regions (such as the hippocampus and amygdala) due to large individual differences are not well distinguished by human-based visual analyses.<sup>58,59</sup> Das *et al.*<sup>60</sup> proposed a machine learning method called 'sparse high-order interaction model with the rejection phenomenon'. Their reported sensitivity, specificity and AUC for AD versus NC were 84.00%, 69.00% and 0.860, respectively, which did not prove superior to our respective CNN outcomes: (99.80%, 98.40% and 0.999), and moreover, imposed a much larger work input burden during image pre-processing. Khazaei *et al.*<sup>61</sup> applied SVM with ADNI MRI images to classify three groups (NC, MCI and AD) with an accuracy of 88.40%, but we are reporting a much higher accuracy outcome of 92.10% in this current study. Furthermore, in their study, their reported classification accuracies for distinguishing NC from AD and MCI, AD from NC and MCI and MCI from NC and AD were 87.30%, 97.50% and 72.00%, respectively. However, in our study, we are reporting classification accuracies of 93.71%, 96.73% and 96.82% for distinguishing NC from AD and

MCI, AD from NC and MCI and MCI from NC and AD, respectively. Although the classification accuracy of AD from NC and MCI is almost equivalent, their other two accuracies were far less; compared to the 3D-CNN-SVM results, we obtained. Compared with the traditional data-driven method, the deep learning method does not necessarily require any time demanding to preprocess steps when selecting the feature, since it is already self-programmed to acquire the best performance for the classification.<sup>62,63</sup> This may be the potential reason why CNN proves superior to machine learning method in the classification of NC, MCI and AD.

Deep learning is rapidly growing in processing neuroimaging data.<sup>64</sup> In recent years, a large number of studies have been reported for their application of CNN in the diagnosis of AD.<sup>31,65</sup> Wang *et al.*<sup>66</sup> proposed an eight-layer CNN with ADNI MRI images and achieved a sensitivity of 97.96%, a specificity of 97.35% and an accuracy of 97.65% for the classification of AD versus NC. In addition, Cui and colleagues<sup>67</sup> also proposed a CNN with ADNI MRI images to achieve a classification accuracy of 91.33% for AD versus NC, whereas in this study, the 3D-CNN-SVM improved the sensitivity, specificity and accuracy to 99.80%, 98.40% and 99.10%, respectively.

Liu *et al.*<sup>68</sup> performed a new classification framework based on a combination of CNN and recurrent neural network (RNN) to compare 3D-CNN by ADNI PET images. The performance of this new classification framework and 3D-CNN reported accuracies of 91.20% and 87.10%, with AUC of 0.953 and 0.935, respectively, for AD versus NC classification, while accuracies of 78.9% and 75.60% with AUC of 0.839 and 0.821 were respectively reported for the MCI versus NC classification. In this study, we achieved an accuracy of 99.1%, with an AUC of 0.999 for AD versus NC classification, and an accuracy of 98.9%, with an AUC of 0.998 for MCI versus NC classification, which show higher outcomes compared to Liu *et al.*'s findings. Ehsan *et al.*<sup>69</sup> employed the 3D-CNN to predict AD status with MRI, the ternary classification accuracy of which was 89.1%; however, our study reports a much higher accuracy outcome of 95.74%. The probable reason why 3D-CNN-SVM performs better image processing than 2D-CNN may be attributed to the properties of 3D

CNN that allows for the extraction of 3D spatial features from the images.<sup>70</sup> In addition, SVMs with low-dimensional data have been demonstrated to achieve good prediction effects, but not necessarily for high-dimensional imaging data.<sup>71</sup> Therefore, our study proposed a new classification design based on the combination of 3D-CNN and SVM to extract 3D features by making SVM the classifier in order to achieve the observed rated performance.

There are some strengths to this study. First, a novel 3D-CNN-SVM was proposed as a model for the classification of AD. Second, 3D-CNN has also been confirmed to be useful for the diagnosis of AD in prior studies but not for the multi-classification of AD. We utilized this ternary classification with MRI modality, which means that our algorithm can assist radiologists and/or imaging technicians with screening and diagnosis without risk of exposure to irradiation. In addition, the performance of 3D-CNN-SVM proves superior to the current models reported in previous studies. Furthermore, 3D-CNN-SVM proved to be efficient by not having to manually perform any prior feature extraction and is totally independent of the variability of imaging protocols and scanners, suggesting that it can potentially be exploited by untrained operators and extended to virtual patient imaging data.

Our study is not without limitations. First, we solely utilized baseline MRI images for the deep learning method, which implies that we did not consider the follow-up MRIs, as well as the prediction of AD outcomes. Second, we did not compare the radiologist-based diagnoses, which ultimately suggests the possibility of discrepancy(ies) in the diagnostic ability between the discussed model of classification and that of the radiologists, in this study design. Third, AD is clinically heterogeneous in nature, which undoubtedly cannot be disputed. Effective diagnostic models should be developed to deal with atypical presentations of AD manifestations, such as those seen with posterior cortical atrophy and variants of primary progressive aphasia. Finally, neurodegeneration due to AD occurs over years, even decades, before its clinical overtness<sup>72</sup>; therefore, future study goals are encouraged to focus on how to revert MCI to normal states, predict AD pathological progression and improve the performance of the diagnosis of AD at automated levels.

AD clearly remains a global health issue amongst the neurodegenerative diseases despite recent and modern technological advancements in the medical field.<sup>73</sup> One preventive approach to mitigate its occurrence and impact can be achieved through screening methods. 3D-CNN-SMV is expected to establish models for AD automation, individualization and early detection, so as to accelerate the application of MRI technology in our mundane practice and to assist, prevent, or halt the pre-clinical and pathological stages of the disease from progressing to MCI and/or AD.

## 5. Conclusion

Findings from this study illustrate that 3D-CNN-SVM is superior to reported classification models for AD-spectrum diagnosis in previously published studies and holds great potential for employing deep learning designs by setting new platforms for medical diagnostic and interventional imaging. These outcomes further indicate that 3D-CNN has the potential to capture 3D context of MRI scans, like amygdale, temporal lobe and para-hippocampal regions, which are associated with AD, while conventional 2D-CNN can only filter scans of 2D local patterns. Finally, this study makes it more practical and easier to screen AD and MCI in a general population at baseline, with the sole purpose of early diagnosis and potential intervention. Due to the current growing interest in value-based health care paradigms in the United States, it will be more fascinating to know that patients can possibly receive early diagnoses following automated clinical imaging evaluations with this trained model, for early intervention and quality outcomes of patients in clinical practice.

## Acknowledgments

In this work, we employed the database of the Alzheimer's Disease Neuroimaging Initiative (ADNI). ADNI was established as a multicenter longitudinal study to identify imaging, clinical, genetic and biochemical biomarkers for the early detection and tracking of AD and MCI. ADNI is the result of \$67 million partnership efforts by both the public and the private sector. Financial support was obtained from the National Institute on Aging, 13 pharmaceutical companies and 2 foundations providing funding through the Foundation for the National

Institutes of Health. The study can be split into three sub-initiatives — ADNI1, ADNI2 and ADNI GO. The initial phase known as ADNI1 included subjects between 55 and 90 years of age from approximately 50 sites across the United States (US) and Canada. ADNI2 and ADNI GO add new participants and funding to the study. The database is made available to researchers around the world and has a broad range of collaborators. The principal investigator (PI) of ADNI, who oversees all aspects, is Dr. Michael Weiner, MD, VA Medical Center and the University of California — San Francisco. For up-to-date information, see [www.adni-info.org](http://www.adni-info.org). We sincerely thank those who participated in data management and analysis. Especially, the help from the friends of ours who sacrifice a lot in this study. We express our profound gratitude to Mr. Krishna Mandalia and Mr. Brandon Yoshida of University of Southern California (USC) for their proofreading contribution to this manuscript. We are also thankful to Deginet Akililu of Capital Medical University for his support in helping to address reviewers' comments during the major review process. This current study was financially supported by The Program of National Natural Science Foundation of China (Serial Number: 81773542) (X. Guo) (Serial Number: 81530087) (F. Zhang). The funding was neither used for the study design nor data collection but to cover for the publication fees.

## References

1. A. Burns and S. Iliffe, Alzheimer's disease, *BMJ* **338** (2009) b158.
2. O. Valenzuela, X. Jiang, A. Carrillo and I. Rojas, Multi-objective genetic algorithms to find most relevant volumes of the brain related to Alzheimer's disease and mild cognitive impairment, *Int. J. Neural Syst.* **28** (2018) 1850022.
3. N. Mammone, C. Ieracitano, H. Adeli, A. Bramanti and F. C. Morabito, Permutation Jaccard distance-based hierarchical clustering to estimate EEG network density modifications in MCI subjects, *IEEE Trans. Neural Netw. Learn Syst.* **10** (2018) 5122–5135.
4. I. Beheshti, H. Demirel, H. Matsuda and Alzheimer's Disease Neuroimaging Initiative, Classification of Alzheimer's disease and prediction of mild cognitive impairment-to-Alzheimer's conversion from structural magnetic resource imaging using feature ranking and a genetic algorithm, *Comput. Biol. Med.* **83** (2017) 109–119.

5. X. Yan, F. Li, S. Chen and J. Jia, Associated factors of total costs of Alzheimer's disease: A cluster-randomized observational study in China, *J. Alzheimers Dis.* **69** (2019) 795–806.
6. B. Pyenson, T. G. Sawhney, C. Steffens, D. Rotter, S. Peschin, J. Scott and E. Jenkins, The real-world medicare costs of alzheimer disease: Considerations for policy and care, *J. Manag Care Spec. Pharm.* **25** (2019) 800–809.
7. M. Sado, A. Ninomiya, R. Shikimoto, B. Ikeda, T. Baba, K. Yoshimura and M. Mimura, The estimated cost of dementia in Japan, the most aged society in the world, *PLoS One* **13** (2018) e0206508.
8. C. Fang, C. Li, M. Cabrerizo, A. Barreto, J. Andrian, N. Rishe, D. Loewenstein, R. Duara and M. Adjouadi, Gaussian discriminant analysis for optimal delineation of mild cognitive impairment in Alzheimer's disease, *Int. J. Neural Syst.* **28** (2018) 1850017.
9. J. P. Amezcuita-Sanchez, N. Mammone, F. C. Morabito, S. Marino and H. Adeli, A novel methodology for automated differential diagnosis of mild cognitive impairment and the Alzheimer's disease using EEG signals, *J. Neurosci. Methods* **322** (2019) 88–95.
10. J. P. Amezcuita-Sanchez, A. Adeli and H. Adeli, A new methodology for automated diagnosis of mild cognitive impairment (MCI) using magnetoencephalography (MEG), *Behav. Brain Res.* **305** (2016) 174–180.
11. T. D. Koepsell and S. E. Monsell, Reversion from mild cognitive impairment to normal or near-normal cognition: Risk factors and prognosis, *Neurology* **79** (2012) 1591–1598.
12. H. Adeli, S. Ghosh-Dastidar and N. Dadmehr, A spatio-temporal wavelet-chaos methodology for EEG-based diagnosis of Alzheimer's disease, *Neurosci. Lett.* **444** (2008) 190–194.
13. H. Adeli, S. Ghosh-Dastidar and N. Dadmehr, Alzheimer's disease: Models of computation and analysis of EEGs, *Clin EEG Neurosci.* **36** (2005) 131–140.
14. M. Niazi, M. Karaman, S. Das, X. J. Zhou, P. Yushkevich and K. Cai, Quantitative MRI of perivascular spaces at 3T for early diagnosis of mild cognitive impairment, *AJNR Am. J. Neuroradiol.* **39** (2018) 1622–1628.
15. A. Kautzky, R. Seiger, A. Hahn, P. Fischer, W. Krampla, S. Kasper, G. G. Kovacs and R. Lanzemberger, Prediction of autopsy verified neuropathological change of Alzheimer's disease using machine learning and MRI, *Front. Aging Neurosci.* **10** (2018) 406.
16. D. Hwang, S. K. Kang, K. Y. Kim, S. Seo, J. C. Paeng, D. S. Lee and J. S. Lee, Generation of PET attenuation map for whole-body time-of-flight (18)F-FDG PET/MRI using a deep neural network trained with simultaneously reconstructed activity and attenuation maps, *J. Nucl. Med.* **8** (2019) 1183–1189.
17. N. Benamrane and N. Belmokhtar, Classification of Alzheimer's disease from 3D structural MRI data, *Int. J. Comput. Appl.* **47** (2012) 40–44.
18. H. I. Suk, S. W. Lee, D. Shen and Alzheimers Disease Neuroimaging Initiative, Hierarchical feature representation and multimodal fusion with deep learning for AD/MCI diagnosis, *Neuroimage* **101** (2014) 569–582.
19. Y. Sun, Z. Dai, Y. Li, C. Sheng, H. Li, X. Wang, X. Chen, Y. He and Y. Han, Subjective cognitive decline: Mapping functional and structural brain changes — A combined resting-state functional and structural MR imaging study, *Radiology* **281** (2016) 185.
20. R. Casanova, R. T. Barnard, S. A. Gaussoin, S. Saldana, K. M. Hayden, J. E. Manson, R. B. Wallace, S. R. Rapp, S. M. Resnick, M. A. Espeland and J. C. Chen, Using high-dimensional machine learning methods to estimate an anatomical risk factor for Alzheimer's disease across imaging databases, *Neuroimage* **183** (2018) 401–411.
21. H. Jang, S. M. Plis, V. D. Calhoun and J. H. Lee, Task-specific feature extraction and classification of fMRI volumes using a deep neural network initialized with a deep belief network: Evaluation using sensorimotor tasks, *Neuroimage* **145** (2017) 314–328.
22. M. Ahmadlou, H. Adeli and A. Adeli, New diagnostic EEG markers of the Alzheimer's disease using visibility graph, *J. Neural. Transm. (Vienna)* **117** (2010) 1099–1109.
23. Z. Sankari, H. Adeli and A. Adeli, Wavelet coherence model for diagnosis of Alzheimer disease, *Clin. EEG Neurosci.* **43** (2012) 268–278.
24. G. Mirzaei, A. Adeli and H. Adeli, Imaging and machine learning techniques for diagnosis of Alzheimer's disease, *Rev. Neurosci.* **27** (2016) 857–870.
25. M. Ahmadlou, A. Adeli, R. Bajo and H. Adeli, Complexity of functional connectivity networks in mild cognitive impairment subjects during a working memory task, *Clin. Neurophysiol.* **125** (2014) 694–702.
26. S. Bhat, U. R. Acharya, N. Dadmehr and H. Adeli, Clinical neurophysiological and automated EEG-based diagnosis of the Alzheimer's disease, *Euro. Neurol.* **74** (2015) 202–210.
27. S. Hulbert and H. Adeli, EEG/MEG- and imaging-based diagnosis of Alzheimer's disease, *Rev. Neurosci.* **24** (2013) 563–576.
28. N. Mammone, S. De Salvo, L. Bonanno, C. Ieracitano, S. Marino, A. Marra, A. Bramanti and F. C. Morabito, Brain network analysis of compressive sensed high-density EEG signals in AD and MCI subjects, *IEEE T. Ind. Inform.* **15** (2018) 527–536.

29. C. Ieracitano, N. Mammone, A. Bramanti, A. Hus-sain and F. C. Morabito, A convolutional neural network approach for classification of dementia stages based on 2D-spectral representation of EEG recordings, *Neurocomputing* **323** (2019) 96–107.
30. T. Zhou, K. H. Thung, X. Zhu and D. Shen, Effective feature learning and fusion of multimodality data using stage-wise deep neural network for dementia diagnosis, *Hum. Brain Mapp.* **40** (2019) 1001–1016.
31. W. Lin, T. Tong, Q. Gao, D. Guo, X. Du, Y. Yang, G. Guo, M. Xiao, M. Du and X. Qu, Convolutional neural networks-based MRI image analysis for the Alzheimer’s disease prediction from mild cognitive impairment, *Front. Neurosci.* **12** (2018) 777.
32. X. Chen, H. Zhang, Y. Gao, C. Y. Wee, G. Li and S. Shen, High-order resting-state functional connectivity network for MCI classification, *Hum. Brain Mapp.* **37** (2016) 3282–3296.
33. M. Liu, D. Cheng, K. Wang and Y. Wang, Multi-modality cascaded convolutional neural networks for Alzheimer’s disease diagnosis, *Neuroinformatics* **16** (2018) 295–308.
34. J. Zhao, M. Zhang, Z. Zhou, J. Chu and F. Cao, Automatic detection and classification of leukocytes using convolutional neural networks, *Med. Biol. Eng. Comput.* **55** (2017) 1287–1301.
35. E. Moradi, A. Pepe, C. Gaser, H. Huttunen and J. Tohka, Machine learning framework for early MRI-based Alzheimer’s conversion prediction in MCI subjects, *Neuroimage* **104** (2015) 398–412.
36. J. Carballido-Gamio, S. Bonaretti, G. J. Kazakia, S. Khosla, S. Majumdar, T. F. Lang and A. J. Burghardt, Statistical parametric mapping of HR-pQCT images: A tool for population-based local comparisons of micro-scale bone features, *Ann. Biomed. Eng.* **45** (2017) 949–962.
37. J. Han, A. Xia, Y. Huang, L. Ni, W. Chen, Z. Jin, S. Yang and F. Jin, Simultaneous visualization of multiple gene expression in single cells using an engineered multicolor reporter toolbox and approach of spectral crosstalk correction, *ACS Synth. Biol.* **11** (2019) 2536–2546.
38. P. Bach, U. Frischknecht, I. Reinhard, N. Bekier, T. Demirakca, G. Ende, S. Vollstadt-Klein, F. Kiefer and D. Hermann, Impaired working memory performance in opioid-dependent patients is related to reduced insula gray matter volume: A voxel-based morphometric study, *Eur. Arch. Psychiatry. Clin. Neurosci.* **17** (2019) 1–10.
39. S. M. E. Sahraeian, R. Liu, B. Lau, K. Podesta, M. Mohiyuddin and H. Y. K. Lam, Deep convolutional neural networks for accurate somatic mutation detection, *Nat. Commun.* **10** (2019) 1041.
40. O. Ronneberger, P. Fischer and T. Brox, U-Net: Convolutional networks for biomedical image segmentation, in *International Conference on Medical Image Computing and Computer-Assisted Intervention*, Vol. 10 (Springer, 2015), pp. 234–241.
41. F.-J. H. Marc’Aurelio Ranzato, Y.-L. Boureau and Y. LeCun, Unsupervised learning of invariant feature hierarchies with applications to object recognition, in *Proc. Computer Vision and Pattern Recognition Conference (CVPR’07)* (IEEE Press, 2007), pp. 1–8.
42. S. Ji, W. Xu, M. Yang and K. Yu, 3D convolutional neural networks for human action recognition, *IEEE Trans. Pattern Anal. Mach. Intell.* **35** (2012) 221–231.
43. J. Zhao, M. Zhang, Z. Zhou, J. Chu and F. Cao, Automatic detection and classification of leukocytes using convolutional neural networks, *Med. Biol. Eng. Comput.* **55** (2017) 1287–1301.
44. J. Kawahara, C. J. Brown, S. P. Miller, B. G. Booth, V. Chau, R. E. Grunau, J. G. Zwicker and G. Hamarneh, BrainNetCNN: Convolutional neural networks for brain networks; towards predicting neurodevelopment, *Neuroimage* **146** (2017) 1038–1049.
45. S. Parisot, S. I. Ktena, E. Ferrante, M. Lee, R. Guerrero, B. Glocker and D. Rueckert, Disease prediction using graph convolutional networks: Application to autism spectrum disorder and Alzheimer’s disease, *Med. Image Anal.* **48** (2018) 117–130.
46. J. M. J. Vonk, M. A. Renteria, V. M. Medina, M. A. Pericak-Vance, G. S. Byrd, J. Haines, A. M. Brickman and J. J. Manly, Education moderates the relation between APOE  $\epsilon 4$  and memory in nondemented non-hispanic black older adults, *J. Alzheimers Dis.* **72** (2019) 1–12.
47. T. C. Eshetie, T. A. Nguyen, M. H. Gillam and L. M. Kalisch Ellett, Medication use for comorbidities in people with Alzheimer’s disease: An Australian population-based study, *Pharmacotherapy* **39** (2019) 1146–1156.
48. J. L. Podcasy and C. N. Epperson, Considering sex and gender in Alzheimer disease and other dementias, *Dialogues Clin. Neurosci.* **18** (2016) 437–446.
49. M. Calabro, L. Mandelli, C. Crisafulli, S. Porcelli, D. Albani, A. Politis, G. N. Papadimitriou, M. Di Nicola, L. Janiri, R. Colombo, G. Martinotti, A. Bello-mo, E. Vieta, S. Bonassi, A. Frustaci, G. Ducci, S. Landi, S. Boccia and A. Serretti, Psychiatric disorders and SLC6A4 gene variants: Possible effects on alcohol dependence and Alzheimer’s disease, *Mol. Biol. Rep.* **1** (2019) 191–200.
50. M. C. Donohue, R. A. Sperling, R. Petersen, C. K. Sun, M. W. Weiner and P. S. Aisen, Association between elevated brain amyloid and subsequent cognitive decline among cognitively normal persons, *JAMA* **317** (2017) 2305–2316.
51. H. I. Suk, S. W. Lee and D. Shen, Latent feature representation with stacked auto-encoder for AD/MCI diagnosis, *Brain Struct. Funct.* **220** (2015) 841–859.

52. S. Liu, S. Liu, W. Cai, H. Che, S. Pujol, R. Kikinis, D. Feng and M. J. Fulham, Multimodal neuroimaging feature learning for multiclass diagnosis of Alzheimer's disease, *IEEE Trans. Biomed. Eng.* **62** (2015) 1132–1140.
53. Z. Sankari and H. Adeli, Probabilistic neural networks for diagnosis of Alzheimer's disease using conventional and wavelet coherence, *J. Neurosci. Methods* **197** (2011) 165–170.
54. Z. Sankari, H. Adeli and A. Adeli, Intrahemispheric, interhemispheric, and distal EEG coherence in Alzheimer's disease, *Clin. Neurophysiol.* **122** (2011) 897–906.
55. P. Peng, M. Li, H. Liu, Y. R. Tian, S. L. Chu, N. Van Halm-Lutterodt, B. Jing and T. Jiang, Brain structure alterations in respect to tobacco consumption and nicotine dependence: A comparative voxel-based morphometry study, *Front. Neuroanat.* **12** (2018) 43.
56. I. Doycheva, J. Cui, P. Nguyen, E. A. Costa, J. Hooker, H. Hofflich, R. Bettencourt, S. Brouha, C. B. Sirlin and R. Loomba, Non-invasive screening of diabetics in primary care for NAFLD and advanced fibrosis by MRI and MRE, *Aliment. Pharmacol. Ther.* **43** (2016) 83–95.
57. J. delEtoile and H. Adeli, Graph theory and brain connectivity in Alzheimer's disease, *Neuroscientist* **23** (2017) 616–626.
58. N. Mammone, L. Bonanno, S. Salvo, S. Marino, P. Bramanti, A. Bramanti and F. C. Morabito, Permutation disalignment index as an indirect, EEG-based, measure of brain connectivity in MCI and AD patients, *Int. J. Neural Syst.* **27** (2017) 1750020.
59. Y. Ouyang and H. Yin, Multi-step time series forecasting with an ensemble of varied length mixture models, *Int. J. Neural Syst.* **28** (2018) 1750053.
60. D. Das, J. Ito, T. Kadowaki and K. Tsuda, An interpretable machine learning model for diagnosis of Alzheimer's disease, *PeerJ* **7** (2019) e6543.
61. A. Khazaei, A. Ebrahimpour and A. Babajani-Feremi, Application of advanced machine learning methods on resting-state fMRI network for identification of mild cognitive impairment and Alzheimer's disease, *Brain Imaging Behav.* **10** (2016) 799–817.
62. J. K. Eshraghian, S. Baek, J. H. Kim, N. Iannella, K. Cho, Y. S. Goo, H. H. C. Iu, S. M. Kang and K. Eshraghian, Formulation and implementation of nonlinear integral equations to model neural dynamics within the vertebrate retina, *Int. J. Neural Syst.* **28** (2018) 1850004.
63. L. Khedher, I. A. Illan, J. M. Gorriz, J. Ramirez, A. Brahim and A. Meyer-Baese, Independent component analysis-support vector machine-based computer-aided diagnosis system for Alzheimer's with visual support, *Int. J. Neural Syst.* **27** (2017) 1650050.
64. H. K. van der Burgh, R. Schmidt, H. J. Westeneng, M. A. de Reus, L. H. van den Berg and M. P. van den Heuvel, Deep learning predictions of survival based on MRI in amyotrophic lateral sclerosis, *Neuroimage Clin.* **13** (2017) 361–369.
65. C. Lian, M. Liu, J. Zhang and D. Shen, Hierarchical fully convolutional network for joint atrophy localization and Alzheimer's disease diagnosis using structural MRI, *IEEE Trans. Pattern Anal. Mach. Intell.* **99** (2018) 1.
66. S. H. Wang, P. Phillips, Y. Sui, B. Liu, M. Yang and H. Cheng, Classification of Alzheimer's disease based on eight-layer convolutional neural network with leaky rectified linear unit and max pooling, *J. Med. Syst.* **42** (2018) 85.
67. R. Cui and M. Liu, RNN-based longitudinal analysis for diagnosis of Alzheimer's disease, *Comput. Med. Imaging Graph* **73** (2019) 1–10.
68. M. Liu, D. Cheng and W. Yan, Classification of Alzheimer's disease by combination of convolutional and recurrent neural networks using FDG-PET images, *Front. Neuroinform.* **12** (2018) 35.
69. E. Hosseini-Asl, R. Keynton and A. El-Baz, 2016, Alzheimer's disease diagnostics by adaptation of 3D convolutional network, in *2016 IEEE International Conference on Image Processing (ICIP)*, Vol. 9 (IEEE, 2016), pp. 126–130.
70. D. Shen, G. Wu and H. I. Suk, Deep learning in medical image analysis, *Annu. Rev. Biomed. Eng.* **19** (2017) 221–248.
71. A. B. R. Shatte, D. M. Hutchinson and S. J. Teague, Machine learning in mental health: A scoping review of methods and applications, *Psychol. Med.* **49** (2019) 1–23.
72. S. Basaia, F. Agosta, L. Wagner, E. Canu, G. Magnani, R. Santangelo, M. Filippi and Alzheimer's Disease Neuroimaging Initiative, Automated classification of Alzheimer's disease and mild cognitive impairment using a single MRI and deep neural networks, *Neuroimage Clin.* **21** (2018) 101645.
73. F. Feng, P. Wang, K. Zhao, B. Zhou, H. Yao, Q. Meng, L. Wang, Z. Zhang, Y. Ding and L. Wang, 2018, Radiomic features of hippocampal subregions in Alzheimer's disease and amnesic mild cognitive impairment, *Front. Aging Neurosci.* **10** (2018) 290–301.